Eur. Phys. J. B **72**, 441–449 (2009)
DOI: 10.1140/epjb/e2009-00367-0

THE EUROPEAN PHYSICAL JOURNAL B

Regular Article

Diffusion in stochastic sandpiles

S.D. da Cunha[1], R.R. Vidigal[2], L.R. da Silva[1], and R. Dickman[2,3,a]

[1] Departamento de Física Teórica e Experimental, Universidade Federal do Rio Grande do Norte, Campus Universitário, National Institute of Science and Technology for Complex Systems, 59072-970 Natal, Rio Grande do Norte, Brazil
[2] Departamento de Física, ICEx, Universidade Federal de Minas Gerais, Caixa Postal 702, 30161-970 Belo Horizonte, Minas Gerais, Brazil
[3] National Institute of Science and Technology for Complex Systems, Caixa Postal 702, 30161-970 Belo Horizonte, Minas Gerais, Brazil

Received 8 June 2009 / Received in final form 17 August 2009
Published online 31 October 2009 –

Abstract. We study diffusion of particles in large-scale simulations of one-dimensional stochastic sandpiles, in both the restricted and unrestricted versions. The results indicate that the diffusion constant scales in the same manner as the activity density, so that it represents an alternative definition of an order parameter. The critical behavior of the unrestricted sandpile is very similar to that of its restricted counterpart, including the fact that a data collapse of the order parameter as a function of the particle density is possible, but with a narrow scaling region. We also develop a series expansion, in inverse powers of the density, for the collective diffusion coefficient in a variant of the stochastic sandpile in which the toppling rate at a site with n particles is $n(n-1)$, and compare the theoretical prediction with simulation results.

PACS. 05.70.Ln Nonequilibrium and irreversible thermodynamics – 05.50.+q Lattice theory and statistics – 05.65.+b Self-organized systems

1 Introduction

Sandpile models are the prime example of self-organized criticality (SOC) [1,2], or scale-invariance in the apparent absence of control parameters [3]. In sandpiles, SOC arises via a control mechanism that forces the system, which possesses an absorbing-state phase transition, to its critical point [4,5]. SOC in a slowly-driven sandpile corresponds to an absorbing-state phase transition in the *conserved* sandpile, which has the same local dynamics, but a fixed number of particles [4,6–10]. Conserved sandpiles are characterized by a nonconserved order parameter (the activity density) which is coupled to a conserved field that does not evolve in regions devoid of activity [11]. This class, known as conserved directed percolation (CDP), is distinct from that of standard directed percolation [12].

In recent years considerable progress has been made in characterizing the critical properties of conserved stochastic sandpiles, although no complete, reliable theory is yet at hand. As is often the case in critical phenomena, theoretical understanding of scaling and universality rests on the analysis of a continuum field theory or Langevin equation (a nonlinear stochastic partial differential equation) that reproduces the phase diagram and captures the fundamental symmetries and conservation laws of the system. Important steps in this direction are the recent numerical studies of a Langevin equation [12,13] for CDP. The critical exponent values reported in reference [12] are in good agreement with those found in simulations of conserved lattice gas (CLG) models [18,19], which exhibit the same symmetries and conservation laws as stochastic sandpiles. The Langevin equation exponents are also consistent with the best available estimates for stochastic sandpiles in two dimensions [12]. There is now good evidence that the one-dimensional stochastic sandpile belongs to the CDP universality class [14,15].

In this work we focus on an aspect of stochastic sandpiles that has received relatively little attention: diffusion. Since the dynamics in sandpile models involves hopping of particles between neighboring sites, one expects the particle diffusion constant D to follow a scaling behavior similar to that of the usual order parameter, namely, the activity density, ρ. (A site is active if it bears two or more particles.) Here D is defined via the relation $\langle(\Delta x)^2\rangle = 2Dt$, where Δx is the particle displacement. We determine the scaling properties of the diffusion constant in extensive Monte Carlo simulations.

Theoretical studies of the particle diffusion coefficient are hampered by the fact that positions of specific particles are not accessible in the usual stochastic description; instead the master equation describes the evolution of the probability distribution on the set of occupation numbers $\{n_i\}$. It is however possible to determine the *collective*

[a] e-mail: dickman@fisica.ufmg.br

diffusion coefficient D_c by studying how a density perturbation $\Delta p \propto e^{ikx}$ relaxes. D_c is related to the relaxation time, τ_k, of this mode via $\tau_k = 1/(D_c k^2)$, in the small-k limit. Using the path-integral based perturbation theory developed in [23], we calculate the first three terms in the expansion of D_c in inverse powers of density p, for the stochastic sandpile in which the toppling rate is $n(n-1)$.

The balance of this paper is organized as follows. In Section 2 we define the three models of interest. Section 3 reports simulation results on D and ρ for two of these models. In Section 4 we develop a series expansion for the collective diffusion coefficient in a third model, and compare the predictions with simulation results. We close in Section 5 with a summary and discussion.

2 Models

We study three versions of the one-dimensional conserved stochastic sandpile, related to Manna's model [20]. In these systems the configuration is defined by the set of occupation variables $n_1, ..., n_L$, giving the number of particles residing at each site on a ring of size L. Sites with $n_i \geq 2$ are *active*, and those with $n_i \leq 1$ are inactive. The evolution consists of a series of *toppling* events, in which particles are transferred from a active site to one or more of its neighbors. All three versions are continuous-time Markov processes, that is, only one site topples at each event. A Markov process of this kind is defined by the configuration space and the set of transition rates (simply called "rates" in what follows) between pairs of configurations. The particular features distinguishing the three models are as follows.

Basic unrestricted model (I) [21]. Each active site has a rate of unity to topple. Thus at each event, the toppling site is chosen at random from the set of N_{act} currently active sites. When site i topples, two particles are transferred from this site to its neighboring sites ($i-1$ and/or $i+1$, under periodic boundary conditions). The two particles jump independently; they jump to the left or to the right with equal probabilities. The time increment Δt corresponding to a given event is the reciprocal of the total transition rate, i.e., $\Delta t = 1/N_{act}$.

Restricted model (II) [14,16]. The dynamics is that of model I except that no site may have more than two particles. If, when a site topples, a particle attempts to jump to a site bearing two particles, it returns to the toppling site.

Modified unrestricted model (III) [23]. The dynamics is that of model I except that the rate at which site i topples is given by $n_i(n_i-1)$. In this case the probability that a given (active) site is the next to topple is $p_i = n_i(n_i-1)/A$, where $A \equiv \sum_j n_j(n_j-1)$ is the total transition rate. In this case the associated time increment is $1/A$.

While somewhat less convenient for simulation, model III is better suited to operator-based theoretical approaches. The effective repulsion between particles in model II is not intended to model any specific interaction between sand grains. Rather, it was introduced so that the system (for a given size) would have a smaller set of configurations, rendering it more convenient for analysis via cluster approximations [24]. As is usual in studies of critical phenomena, it is of interest to test whether changes in the details of the process, such as the height restriction of model II, have any effect on critical exponents. There is clear numerical evidence that model II belongs to the CDP universality class [14]; models I and III share the same symmetries and conserved quantities as model II and so are expected to belong to the CDP class as well.

In conserved sandpiles, the particle density p serves as a temperaturelike control parameter. Below a certain critical value, p_c, the system eventually falls into an absorbing configuration (i.e., one devoid of active sites), while for $p > p_c$, activity continues indefinitely, in the infinite-size limit. The order parameter associated with this absorbing-state phase transition is the activity density ρ, given by the stationary mean fraction of active sites in models I and II, and the stationary average $\langle n_i(n_i-1)\rangle$ in model III. Numerical studies strongly support a continuous transition at p_c; best estimates for the critical density p_c are 0.9488, 0.92978, and 0.9493, in models I, II, and II, respectively. (Note that for $p > 1$ active sites always exist; p_c, however, is strictly less than unity.)

3 Simulation results

In this section we report simulation results for the particle diffusion rate D and the activity density ρ in models I and II. For each particle j, let $\Delta x_j(t) = h_j^+(t) - h_j^-(t)$ represent its displacement since time zero, where $h_j^+(t)$ and $h_j^-(t)$ are the numbers of hops taken by particle j in the positive (respectively, negative) directions up to time t. (Naturally, $h_j^+(0) = h_j^-(0) = 0$.) Then the particle diffusion rate is defined through the relation

$$\langle [\Delta x_j(t)]^2 \rangle = 2Dt \tag{1}$$

where the average is over all particles and (in principle) all histories of the system of $N = pL$ particles on L sites, starting from a given initial configuration or class of configurations. (In practice we generate initial configurations by adding particles randomly to the system, with the prohibition, in the case of model II, of triple or higher occupancy. We average over a set of N_s realizations of the process.) Note that the diffusion rate D defined above depends in general on the time t as well as on L and p. Determination of D in simulations requires that we store the particle displacements, which is not necessary if we merely wish to study the activity density.

Each time particle j hops, Δx_j changes by ± 1, so that $\langle [\Delta x_j(t)]^2 \rangle = \langle h_j^+(t) + h_j^-(t) \rangle \equiv \langle h_j(t) \rangle$, i.e., the mean number of jumps up to time t. Particle j must be at an active site in order to jump, but $\langle h_j(t) \rangle$ is not simply equal to 2ρ, as would be the case if particle j were always to jump each time the site it resides at topples. In model I, for example, the probability of a given particle jumping is $2/n$, if it is one of n particles at the toppling site. In

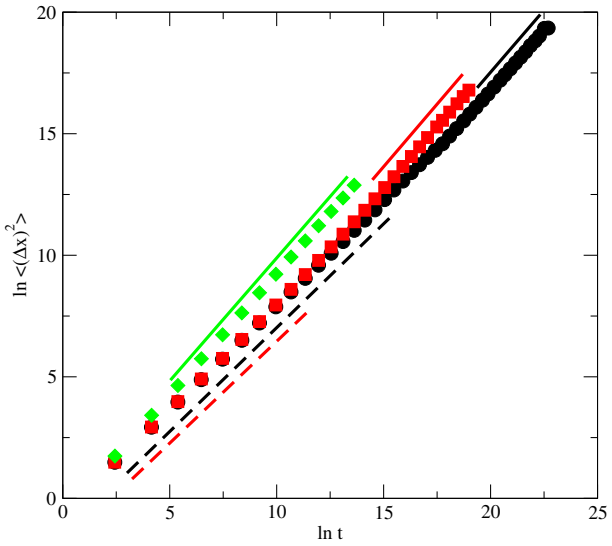

Fig. 1. (Color online) Mean-square particle displacement versus time in model I, for (left to right) $p = 1.94894$, 0.95568, and 0.94898. The solid lines have a slope of unity; the slope of the broken lines is 0.86. Error bars are smaller than the symbols.

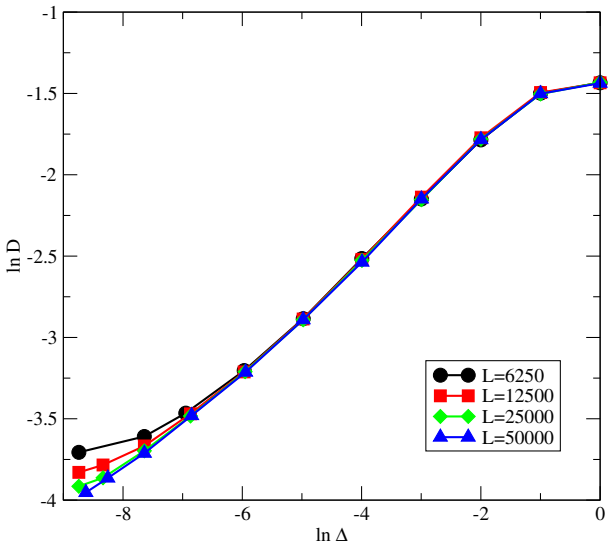

Fig. 2. (Color online) Asymptotic diffusion rate versus $\Delta = p - p_c$ in model I, system sizes as indicated. Error bars are smaller than the symbols.

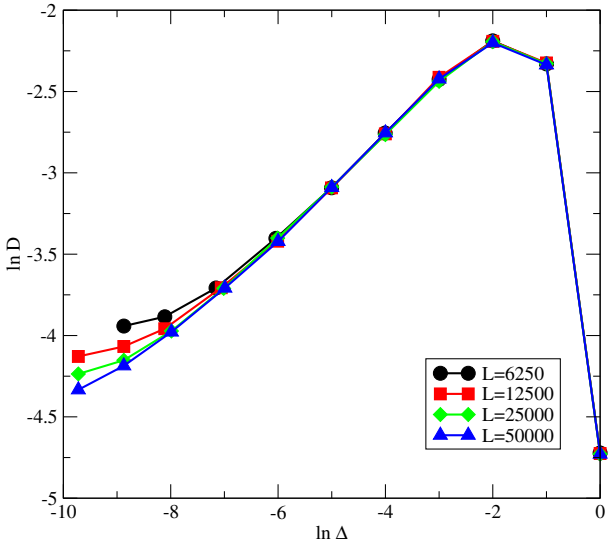

Fig. 3. (Color online) Asymptotic diffusion rate versus Δ in model II.

model II, the particle always tries to hop when its host site topples, by it may be unable to move to the target site. Finally, in model III a particle at a site with occupation n hops at a rate of $2(n-1)$, so that the hopping rate actually grows with the occupation number n. Since the occupancies of nearby sites are correlated, the waiting times between successive displacements of a given particle are not independent. For these reasons, the relation between the hopping rate and the activity density involves subtle effects, different in each of the three models studied. It is nevertheless reasonable to expect that, as $p \to p_c$, the scaling behavior of the diffusion rate will parallel that of the activity density. In particular, we might expect ρ and D to be governed by the same set of critical exponents at the transition.

We simulate models I and II on rings of $L = 6250$, 12 500, 25 000, and 50 000 sites, using eight independent realizations for the smallest size, six for $L = 12\,500$, and four for the two largest sizes. The studies are run for 10^6 to 6×10^9 time units, with the longest simulation times near the critical point. Each particle is assigned a label so that its cumulative dislocation Δx_j can be followed during the evolution. In model II, when two particles attempt to jump to the same site, and this site is singly occupied, one of the two particles is chosen at random to move to the target site, while the other remains where it is.

To begin, we verify that the mean-square particle displacement indeed grows linearly with time in the stationary regime. This is confirmed for model I in Figure 1 for three values of the particle density p. (These data are for system size $L = 50\,000$ and represent an average over four independent runs.) The relation $\langle[\Delta x_j(t)]^2\rangle \propto t$ is similarly confirmed in model II. We note that in both models I and II, near the critical point, the mean-square particle displacement initially grows more slowly, following $\langle[\Delta x_j(t)]^2\rangle \propto t^\gamma$, with $\gamma = 0.86(1)$ (see Fig. 1).

We monitor the diffusion coefficient $D(t)$, defined in equation (1), and confirm that it approaches a stationary value at long times. Figures 2 and 3 show the stationary value, D, as a function of $\Delta = p - p_c$, for models I and II, respectively. Several aspects of these results are worth commenting on. First, for the sizes considered here, D is apparently well converged to its limiting ($L \to \infty$) value for $\Delta \geq 0.0025$. Second, even for values of Δ such that the diffusion rate has converged, the slope of $D(\Delta)$ on logarithmic scales changes appreciably with Δ, making a reliable estimate of β difficult. Finally, in model II, D drops sharply as p approaches 2: due to the height restriction, most particles cannot move.

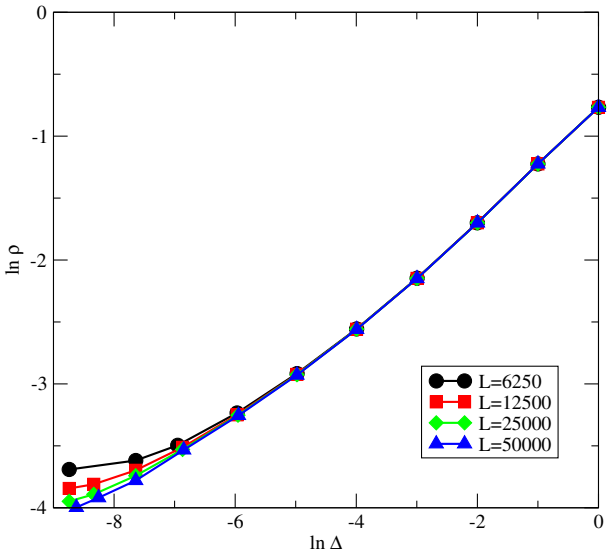

Fig. 4. (Color online) Stationary activity density ρ versus Δ in model I.

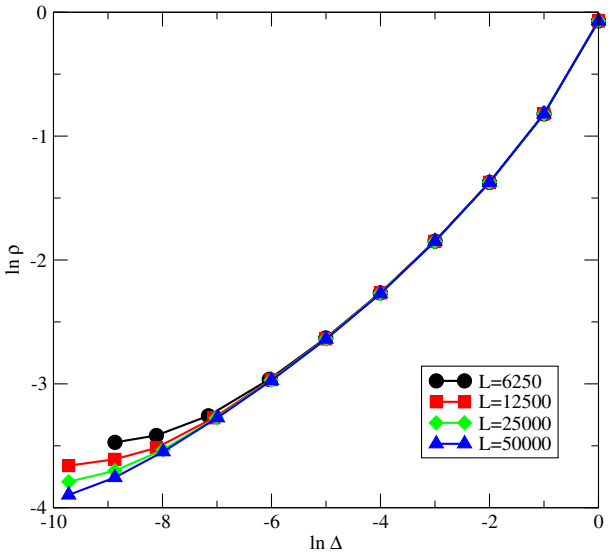

Fig. 5. (Color online) Stationary activity versus Δ in model II.

The corresponding results for the activity density ρ are shown in Figures 4 and 5, respectively. The behaviors of D and ρ in both models appear quite similar, an impression that is confirmed in Figure 6, which compares both quantities (in both models), for the largest system studied. Near the transition, ρ and D are virtually identical in the unrestricted model, while in model II they appear to be proportional. It is evident that neither ρ nor D can be characterized as following a simple power law, an observation already made for the order parameter in model II in [14].

Note that for the system sizes studied here, there is no discernable finite-size effect for $p - p_c \geq 0.0025$. Since $D(\Delta)$ and $\rho(\Delta)$ do not follow simple power laws in this regime, there is no possibility of maintaining the data collapse under the usual kind of FSS scaling plot, that is,

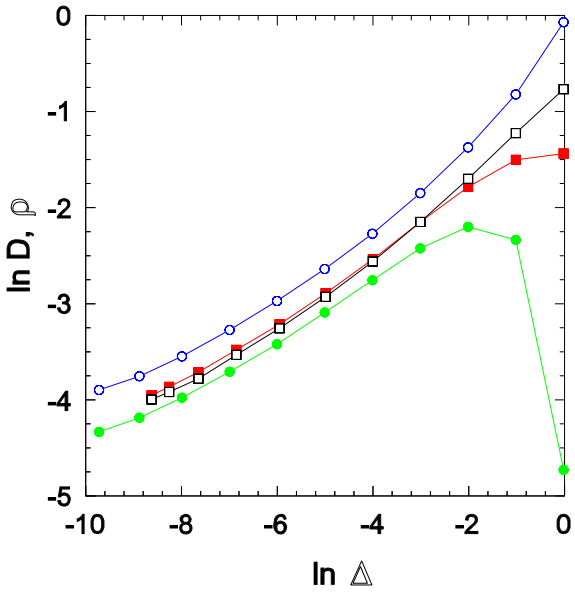

Fig. 6. (Color online) Stationary activity (open symbols) and asymptotic diffusion rate (filled symbols) versus Δ in models I (squares) and II (circles), system size $L = 50\,000$.

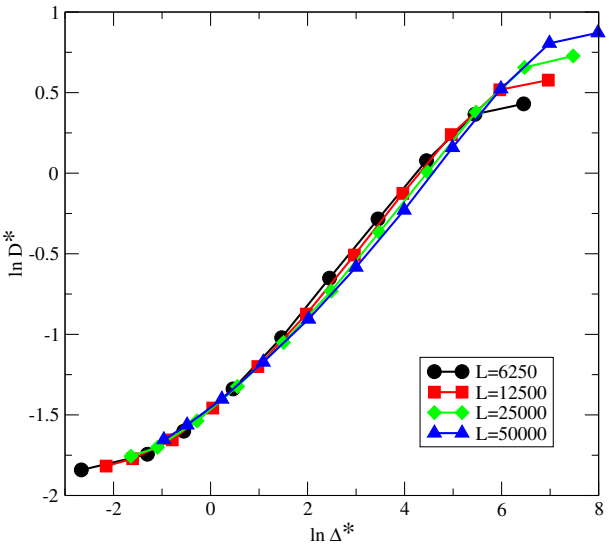

Fig. 7. (Color online) Scaled diffusion rate $D^* = L^{\beta/\nu_\perp} D$ versus scaled distance from critical point $\Delta^* = L^{1/\nu_\perp} \Delta$ in model I.

of $\rho^* = L^{\beta/\nu_\perp} \rho$ versus $\Delta^* = L^{1/\nu_\perp} \Delta$. As noted in [14], a data collapse can only be achieved in the regime very near the critical point (i.e., $\Delta \leq 0.0025$); and example of a data collapse for the diffusion rate data is shown in Figure 7. In model I the data collapse is best using exponent values $\beta = 0.289$ and $\nu_\perp = 1.35$; the corresponding values in model II are $\beta = 0.285$ and $\nu_\perp = 1.355$. These values are consistent with those reported in [14]: $\beta = 0.289(12)$ and $\nu_\perp = 1.355(18)$. We may therefore affirm, with a high degree of confidence, that models I and II belong to the same universality class, and that the diffusion rate and the order parameter exhibit the same critical scaling properties.

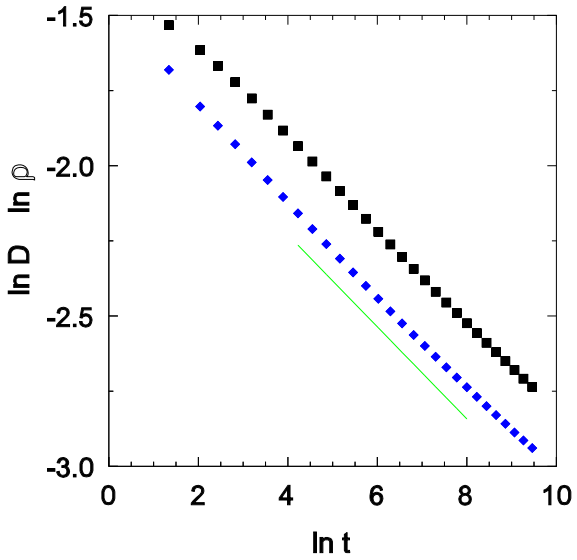

Fig. 8. (Color online) Initial decay of activity (upper) and diffusion rate (lower) at criticality in model I; system size $L = 50\,000$. The slope of the straight line is –0.153.

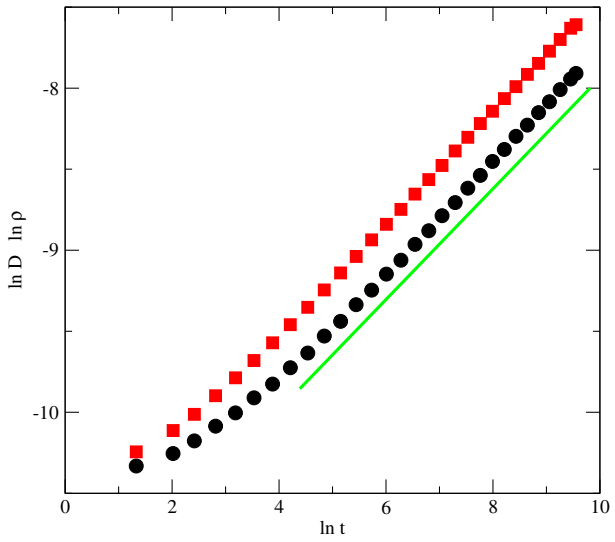

Fig. 9. (Color online) Initial growth of activity (squares) and diffusion rate (circles) at criticality in model II, starting with a single active site; system size $L = 50\,000$. The slope of the straight line is 0.347.

In the paradigmatic examples of absorbing-state phase transitions, such as the contact process [25,26], starting from a spatially homogeneous initial distribution, the order parameter exhibits an initial power-law decay, $\rho \sim t^{-\delta}$, at the critical point, before saturating at a quasistationary value. (Note that the power-law portion of the evolution is independent of system size.) It is of interest to know whether the order parameter and the diffusion rate exhibit similar behavior in the stochastic sandpile. Our results (Fig. 8) for $L = 50\,000$ show ρ and D decaying with an exponent $\delta = 0.153(5)$.

We also perform simulations of the spread of activity with time. In this case, a single site is given two particles initially, while the remaining $N - 2$ particles are distributed at random, one per site, over the rest of the lattice. In the contact process at criticality, starting with a single active site, the number of active sites grows as $n(t) \sim t^{\eta}$, while the mean-square distance of active sites from the original seed grows as $R^2(t) \sim t^{z_{sp}}$ [25,26]. In the present case we find that both D and ρ follow an approximate power law with an exponent $\eta = 0.35(1)$, as shown in Figure 9. The spreading exponents δ, η, and z_{sp} are expected to satisfy the hyperscaling relation $4\delta + 2\eta = dz_{sp}$, which, using $z_{sp} = 2/z$, with z the usual dynamic exponent, can be written as $\eta = 1/z - 2\delta$. Using the value of δ cited above, and $z = 1.50(4)$ from reference [14], this yields $\eta = 0.36(3)$, which is consistent with our numerical estimate.

4 Collective diffusion coefficient: theory and simulation

In this section we apply the operator formalism and perturbation theory derived in [23] to the evaluation of the collective diffusion coefficient D_c of model III on a ring of N sites. We begin by writing the master equation for the process in the form

$$\frac{d|\Psi\rangle}{dt} = L|\Psi\rangle, \tag{2}$$

where

$$|\Psi\rangle = \sum_{\{n\}} p(\{n\}, t)|\{n\}\rangle \tag{3}$$

is the probability distribution. Here $p(\{n\}, t)$ is the probability of configuration $\{n\}$, and the state $|\{n\}\rangle$ is a direct product of states $|n_j\rangle$, representing exactly n_j particles at site j. These states are normalized so: $\langle n'|n\rangle = n!\delta_{n,n'}$.

Defining creation and annihilation operators via the relations,

$$a_i|n_i\rangle = n_i|n_i - 1\rangle \tag{4}$$

and

$$\pi_i|n_i\rangle = |n_i + 1\rangle, \tag{5}$$

so that $[a_i, \pi_j] = \delta_{ij}$, the evolution operator for the one-dimensional stochastic sandpile is

$$L = \sum_i \left[\frac{1}{4}(\pi_{i-1} + \pi_{i+1})^2 - \pi_i^2\right] a_i^2. \tag{6}$$

Since the system is translation-invariant it is convenient to introduce the discrete Fourier transform via

$$a_k = \sum_j e^{-ijk} a_j, \tag{7}$$

with inverse

$$a_j = \frac{1}{N} \sum_k e^{ijk} a_k, \tag{8}$$

(and similarly for other variables), where the allowed values of the wavevector are:

$$k = -\pi,\ -\pi+\frac{2\pi}{N},\ldots-\frac{2\pi}{N},\ 0,\ \frac{2\pi}{N},\ldots,\pi-\frac{2\pi}{N}. \quad (9)$$

(To avoid heavy notation, we indicate the Fourier transform by the subscript k; the subscript j denotes the corresponding variable on the lattice). In the Fourier representation, the evolution operator takes the form

$$L = -N^{-3}\sum_{k_1,k_2,k_3}\omega_{k_1,k_2}\pi_{k_1}\pi_{k_2}a_{k_3}a_{-k_1-k_2-k_3}, \quad (10)$$

where $\omega_{k_1,k_2} = 1-\cos k_1\cos k_2$. As explained in reference [23], the evolution operator may be rewritten as

$$L = L_0 + L_1 \quad (11)$$

with

$$L_0 = -N^{-1}\sum_{k\neq 0}\gamma_k\pi_{-k}a_k, \quad (12)$$

and

$$\begin{aligned}L_1 = &-N^{-3}\sum_{k_1,k_2,k_3\neq 0}\omega_{k_3,-k_1-k_2-k_3}\pi_{k_3}\pi_{-k_1-k_2-k_3}a_{k_1}a_{k_2}\\ &-2pN^{-2}\sum_{k_1,k_2\neq 0}\omega_{k_2,-k_1-k_2}\pi_{k_2}\pi_{-k_1-k_2}a_{k_1}\\ &-2N^{-2}\sum_{k_1,k_2\neq 0}\omega_{-k_1-k_2,0}\pi_{-k_1-k_2}a_{k_1}a_{k_2}\\ &-p^2N^{-1}\sum_{k\neq 0}\omega_{k,-k}\pi_k\pi_{-k}, \end{aligned}\quad (13)$$

where

$$\gamma_k = 4p\,\omega_{k,0} = 4p(1-\cos k). \quad (14)$$

This transformation is based on the observation that, due to particle conservation, the operator $N^{-1}\sum_j\pi_j a_j$ may be equated to the particle density p. In equation (13), it is understood that none of the wavevectors associated with the operators a and π may be zero.

Let $P_n = e^{-p}p^n/n!$ denote the Poisson distribution with intensity p, and define $|P\rangle_i = \sum_n P_n|n\rangle_i$ as the Poisson-distributed state at site i. Then the uniform product-Poisson distribution is $|P\rangle \equiv \otimes_i|P\rangle_i$. The latter is an eigenstate of the diffusion operator with eigenvalue zero, i.e., $\mathcal{D}|P\rangle = 0$, where

$$\begin{aligned}\mathcal{D} &= \frac{1}{2}\sum_j\left[\pi_{j-1}-2\pi_j+\pi_{j+1}\right]a_j\\ &= -N^{-1}\sum_k\omega_{k,0}\pi_{-k}a_k, \end{aligned}\quad (15)$$

represents nearest-neighbor hopping at unit rate. (Note that $L_0 = 4p\mathcal{D}$.)

To study collective diffusion, we consider an initial condition in which the uniform Poisson-product is weakly perturbed by a density modulation with wavevector k:

$$|\Psi(0)\rangle = N^{-1}\pi_k|P\rangle. \quad (16)$$

Introducing the notation,

$$\langle\ |\equiv\sum_{\{n\}}\prod_j\frac{1}{n_j!}\langle n_j| \quad (17)$$

for the projection onto all possible configurations, the mean number of particles at site j is given by

$$\phi_j(t) = \langle n_j(t)\rangle = \langle\ |a_j|\Psi(t)\rangle \quad (18)$$

or equivalently, in the Fourier representation,

$$\phi_k(t) = \langle\ |a_k|\Psi(t)\rangle. \quad (19)$$

Note that for the initial distribution of equation (16), with $k\neq 0$, we have

$$N^{-1}\langle\ |a_q\pi_k|P\rangle = \delta_{q,-k} \quad (20)$$

where we used the relations $[a_q,\pi_k] = N\delta_{q,-k}$ and $\langle\ |\pi_k|P\rangle = N\delta_{k,0}$. Thus $\phi_{-k}(t)$ represents the amplitude, at time t, of the density perturbation created at time zero.

We assume that for long times and long wavelengths the mean density ϕ_j satisfies the diffusion equation $\partial\phi_j/\partial t = D_c\Delta^2\phi_j$ with Δ^2 the discrete Laplacian, leading, in the small-k limit, to $\phi_k(t)\simeq\phi_k(0)\exp[-D_ck^2t]$. Letting $\phi_k(z)$ denote the Laplace transform, we have, in the small-z limit, $\phi_k(z)\simeq 1/(z+D_ck^2)$, so that,

$$D_c = \lim_{k,z\to 0}\frac{1}{k^2\phi_k(z)}. \quad (21)$$

Laplace transforming the formal solution of the master equation we find

$$\phi_{-k} = N^{-1}\langle\ |a_{-k}\frac{1}{z-L}\pi_k|P\rangle. \quad (22)$$

We may develop the solution in a series in powers of $1/p$ using the operator identity

$$\begin{aligned}\frac{1}{z-L_0-L_1} = &\frac{1}{z-L_0}+\frac{1}{z-L_0}L_1\frac{1}{z-L_0}\\ &+\frac{1}{z-L_0}L_1\frac{1}{z-L_0}L_1\frac{1}{z-L_0}+\cdots\end{aligned}\quad (23)$$

Evaluation of the contributions to this series is facilitated by use of the identities $L_0|P\rangle = 0$, $a_k|P\rangle = Np\delta_{k,0}|P\rangle$, and,

$$\langle\ |a_q\pi_k|P\rangle = N\delta_{q,-k}+N^2p\delta_{q,0}\delta_{k,0}. \quad (24)$$

Note also that $L_0\pi_k|p\rangle = -\gamma_k\pi_k|P\rangle$, and in general,

$$L_0\,\pi_{k_1}\cdots\pi_{k_n}|P\rangle = -\mathcal{S}\,\pi_{k_1}\cdots\pi_{k_n}|P\rangle \quad (25)$$

where $\mathcal{S} = \gamma_{k_1}+\cdots+\gamma_{k_n}$. Thus L_0 may be inverted on the space of states of the form $\pi_{k_1}\cdots\pi_{k_n}|P\rangle$ provided that not all of the wave vectors are zero: on this space L_0^{-1} is simply $-1/\mathcal{S}$ times the identity operator.

The first term in the expansion of equation (22) is readily evaluated as,

$$\phi^{(0)}_{-k} = N^{-1}\langle\ |a_{-k}\frac{1}{z-L_0}\pi_k|P\rangle = \frac{1}{z+\gamma_k}, \quad (26)$$

which gives $\lim_{k,z\to 0}\, k^2\phi_{-k}(z) = 1/(2p)+\mathcal{O}(1/p^2)$. Subsequent terms in the expansion may be evaluated using the diagrammatic perturbation approach developed in [23]. In this representation each term in L_1 corresponds to a vertex, with operators a_k corresponding to lines entering the vertex at the right, and operators π_k to lines leaving at the left. Each line that leaves a vertex must be joined ("contracted") with a line entering some other vertex to the left. The operator L_1, equation (13), consists of four parts or vertices, designated respectively as a crossing (two lines in, two out), a bifurcation (one in, two out), a conjunction, and a source. We denote these contributions as L_a, L_b, L_c and L_d, respectively. There are two diagrams that contribute to $\phi_{-k}(z)$ at order $1/p^2$. One arises from the term,

$$N^{-1}\langle\, |a_{-k}\frac{1}{z-L_0}L_c\frac{1}{z-L_0}L_b\frac{1}{z-L_0}\pi_k|P\rangle = \frac{1}{8Np^2(1-\cos k)} \times \sum_{q\neq 0}\frac{1-\cos q\cos(k-q)}{2-\cos q-\cos(k-q)} = \frac{1}{16p^2(1-\cos k)}, \quad (27)$$

while the second is,

$$N^{-1}\langle\, |a_{-k}\frac{1}{z-L_0}L_c\frac{1}{z-L_0}L_c\frac{1}{z-L_0}L_d\frac{1}{z-L_0}\pi_k|P\rangle = -\frac{1}{32p^2(1-\cos k)} \quad (28)$$

where in both cases the limit $z\to 0$ is taken, as required by equation (21). At order $1/p^3$ there are 17 diagrams, leading to

$$D_c = \frac{2p}{1+\frac{1}{8p}+\frac{0.1088899}{p^2}+\cdots}. \quad (29)$$

In [23] the stationary activity density $\rho = \langle n(n-1)\rangle$ was found to grow asymptotically as p^2, with corrections in inverse powers of p; here we find that D_c grows only linearly with p. For comparison we write the results for ρ and D_c in the form:

$$\rho = p^2\left[1-\frac{1}{4p}-\frac{0.0492525}{p^2}+\cdots\right] \quad (30)$$

and

$$D_c = 2p\left[1-\frac{1}{8p}-\frac{0.093265}{p^2}+\cdots\right]. \quad (31)$$

These expressions are reliable for $4p \gg 1$ but cannot of course be applied in the vicinity of the critical density, $p_c \simeq 0.9493$.

4.1 Comparison with simulation

We determine the collective diffusion coefficient in model III via analysis of the *projection* of the configuration $\{n(j,t)\}$ on the initial configuration. Recalling that $\langle n_j(t)\rangle = p$, the particle density, we let $f_j(t) \equiv n_j(t) - p$ denote the excess particle number at site j and time t. Initially, the $\{n_j\}$ are independent, Poisson-distributed with mean p. Consider now

$$\Phi(t) \equiv \frac{\langle f_j(t)f_j(0)\rangle}{\langle f_j(0)^2\rangle} \quad (32)$$

where the angular brackets denote an average over sites and over realizations, including the random initial configuration. For the set of wavevectors k defined in equation (9), let $\varphi_k(t)$ denote the discrete Fourier transform,

$$\varphi_k(t) = \sum_{j=1}^{N} f_j(t)e^{ijk}. \quad (33)$$

In the small-k limit we expect φ_k to follow,

$$\varphi_k(t) = \varphi_k(0)e^{-D_c k^2 t}. \quad (34)$$

Using the fact that the $f_j(0)$ are independent, zero-mean random variables with $\mathrm{var}[f_j(0)] = p$, it is straightforward to show that

$$\Phi(t) = \frac{1}{N}\sum_k e^{-D_c k^2 t} \simeq \frac{1}{2\pi}\int_{-\pi}^{\pi} e^{-D_c k^2 t}dk. \quad (35)$$

For times such that $D_c\pi^2 t \gg 1$ we may extend the limits of integration to $\pm\infty$, yielding

$$\Phi \simeq \frac{1}{2\pi}\sqrt{\frac{\pi}{D_c t}}. \quad (36)$$

Thus if $\Phi(t)$, as determined via simulation, can be fit for large t with an expression of the form $A/t^{1/2}$, then $D_c = 1/(4\pi A^2)$. In practice, however, a more reliable procedure is to fit the simulation data to the full lattice expression

$$\mathcal{F}(t) \equiv \frac{1}{N}\sum_k e^{-2D_c[1-\cos k]t} \quad (37)$$

which involves the single adjustable parameter D_c, and is capable of fitting the data at short as well as long times, and for various system sizes.

We determine $\Phi(t)$ on rings of $N = 200, 400, 800, ..., 25\,600$ sites, for particle densities p in the range of 1 to 3. Figure 10 shows that as the system size increases, $\Phi(t)$ approaches a power-law decay with an exponent of 1/2; an example of data fit by equation (37) is shown in Figuare 11. The estimates for D_c, obtained by fitting $\mathcal{F}(t)$ to the simulation data, are compared with the theoretical prediction, equation (29), in Figure 12; the agreement is quite good for densities $p \geq 2$. In Figure 12, the relatively large error bars associated with the simulation results for $p = 1.1$ and 1.2 reflect the fact that the simulation results for $\Phi(t)$ are less well fit by the theoretical expression, equation (37), than for other particle densities. Curiously, for $p = 1$, despite being nearer the critical point, the fit is again quite good.

A similar analysis can be applied to extract the value of $D_{c,s}$ from simulations in the stationary state. In this case,

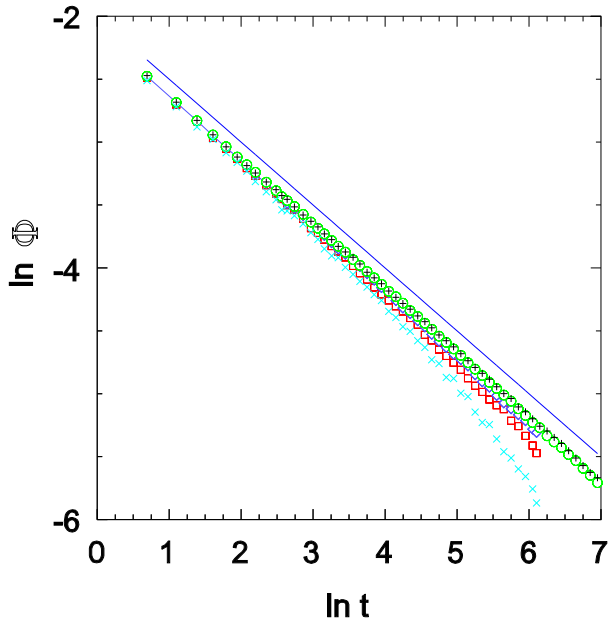

Fig. 10. (Color online) Projection $\Phi(t)$ in simulations of model III. System sizes (lower to upper) $N = 400$, 800,..., 6400, particle density $p = 3.0$. The slope of the straight line is $-1/2$.

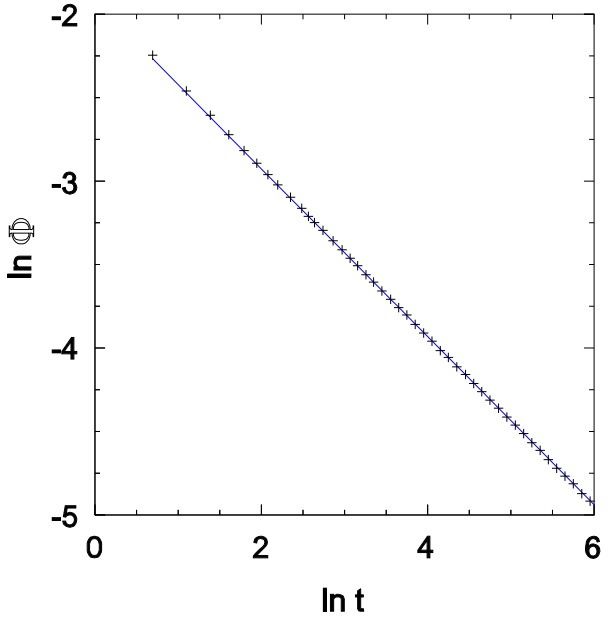

Fig. 11. (Color online) Projection $\Phi(t)$ in simulations of model III with $N = 12\,800$ and $p = 2.0$. The solid line is given by equation (37) with $D_c = 3.76$.

we allow the system to relax, so that the configuration at time zero is typical of the stationary distribution. Now, however, the $f_j(0)$ are no longer independent, Poisson distributed variables, and the power spectrum of fluctuations $\langle|\varphi_k(0)|^2\rangle$ is no longer constant. We therefore fit the data for $\Phi(t)$ using the expression

$$\mathcal{F}_s(t) \equiv \frac{\sum_k \langle|\varphi_k(0)|^2\rangle e^{-2D_{c,s}[1-\cos k]t}}{\sum_k \langle|\varphi_k(0)|^2\rangle} \qquad (38)$$

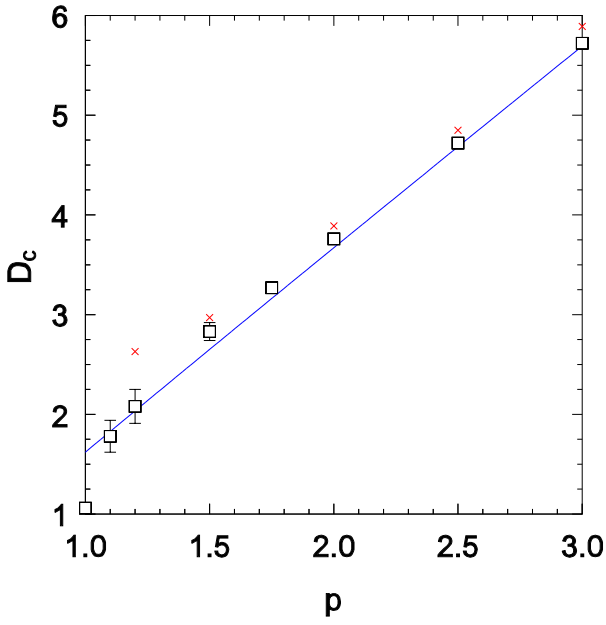

Fig. 12. (Color online) Collective diffusion constant D_c versus particle density p in model III. Squares: simulation; line: theory, equation (29). The crosses denote simulation values for the stationary-state collective diffusion constant $D_{c,s}$.

with $\langle|\phi_k(0)|^2\rangle$ determined via simulation. The resulting stationary values of $D_{c,s}$ are close to, but slightly greater than, those found using the Poisson initial distribution (see Fig. 12). It is worth noting that in the stationary state the projection $\Phi(t)$ appears to decay with a power smaller than 1/2 (a typical exponent value is about 0.41). This does not imply anomalous behavior as the data can again be fit using the hypothesis $\varphi_k(t) = \varphi_k(0)e^{-D_c k^2 t}$. For densities $p < 1.2$ however, the simulation data are not well fit by the function $\mathcal{F}_s(t)$. In this regime the Fourier amplitudes $\langle\varphi_{-k}(t)\varphi_k(0)\rangle$ (calculated in simulations) do not follow a simple exponential decay. (The data suggest a crossover to stretched-exponential decay at long times). Thus, near the critical point, we find evidence of anomalous relaxation, as previously noted in stochastic sandpiles [27].

5 Summary

We study diffusion in stochastic sandpiles. In the first part of this work we determine the particle diffusion coefficient in sandpiles in which all active sites share the same toppling rate. We find, in both the restricted and unrestricted cases, that the diffusion constant scales in the same manner as the order parameter (the activity density). Such a proportionality between the diffusion constant and the activity density was asserted for Abelian sandpiles by Dhar and Pradhan [28]. Our results confirm that the restricted and unrestricted models belong to the same universality class, and that both models exhibit a finite-size scaling collapse of data over an unusually narrow region of the control parameter (that is, the particle density p).

The second part of this study deals with a sandpile in which the toppling rate at site i is $n_i(n_i - 1)$. In this case it is possible to derive a short series for the collective diffusion constant, starting from a Poisson-product initial state. The resulting expression compares well with simulation for densities well above p_c. The collective diffusion constant D_c is extracted from simulations using the projection of density fluctuations at time t onto their initial values. We expect this approach to be useful in determining D_c in other systems, such as interacting lattice gases. We defer a detailed investigation of collective diffusion in the critical region to future work.

We thank Alvaro Vianna Novaes de Carvalho Teixeira for helpful discussions during the initial phase of this study. This work was supported by CNPq and Fapemig, Brazil.

References

1. P. Bak, C. Tang, K. Wiesenfeld, Phys. Rev. Lett. **59**, 381 (1987); P. Bak, C. Tang, K. Wiesenfeld, Phys. Rev. A **38**, 364 (1988)
2. D. Dhar, Physica A **263**, 4 (1999), and references therein
3. G. Grinstein, in *Scale Invariance, Interfaces and Nonequilibrium Dynamics*, edited by A. McKane et al., NATO Advanced Study Institute (Plenum, New York, 1995), Series B: Physics, Vol. 344
4. R. Dickman, M.A. Muñoz, A. Vespignani, S. Zapperi, Braz. J. Phys. **30**, 27 (2000)
5. M.A. Muñoz, R. Dickman, R. Pastor-Satorras, A. Vespignani, S. Zapperi, in *Modeling Complex Systems*, edited by J. Marro, P.L. Garrido, *Proceedings of the 6th Granada Seminar on Computational Physics*, AIP Conference Proceedings **574** (2001)
6. C. Tang, P. Bak, Phys. Rev. Lett. **60**, 2347 (1988)
7. M. Paczuski, S. Maslov, P. Bak, Phys. Rev. E **53**, 414 (1996)
8. A. Vespignani, S. Zapperi, Phys. Rev. Lett. **78**, 4793 (1997); A. Vespignani, S. Zapperi, Phys. Rev. E **57**, 6345 (1998)
9. R. Dickman, A. Vespignani, S. Zapperi, Phys. Rev. E **57**, 5095 (1998)
10. A. Vespignani, R. Dickman, M.A. Muñoz, S. Zapperi, Phys. Rev. Lett. **81**, 5676 (1998)
11. M. Rossi, R. Pastor-Satorras, A. Vespignani, Phys. Rev. Lett. **85**, 1803 (2000)
12. J.J. Ramasco, M.A. Muñoz, C.A. da Silva Santos, Phys. Rev. E **69**, R045105 (2004)
13. I. Dornic, H. Chaté, M.A. Muñoz, Phys. Rev. Lett. **94**, 100601 (2005)
14. R. Dickman, Phys. Rev. E **73**, 036131 (2006)
15. J.A. Bonachela, M.A. Muñoz, Phys. Rev. E **78**, 041102 (2008)
16. R. Dickman, T. Tomé, M.J. de Oliveira, Phys. Rev. E **66**, 016111 (2002)
17. S. Lübeck, Phys. Rev. E **66**, 046114 (2002)
18. R. Pastor-Satorras, A. Vespignani, Phys. Rev. E **62**, R5875 (2000)
19. J. Kockelkoren, H. Chaté, e-print arXiv:cond-mat/0306039
20. S.S. Manna, J. Stat. Phys. **59**, 509 (1990); S.S. Manna, J. Phys. A **24**, L363 (1991)
21. R. Dickman, M. Alava, M.A. Muñoz, J. Peltola, A. Vespignani, S. Zapperi, Phys. Rev. E **64**, 056104 (2001)
22. S. Lübeck, P.C. Heger, Phys. Rev. E **68**, 056102 (2003)
23. R.R. Vidigal, R. Dickman, J. Stat. Phys. **118**, 1 (2005)
24. R. Dickman, Phys. Rev. E **66**, 036122 (2002)
25. P. Grassberger, A. de la Torre, Ann. Phys. (N.Y.) **122**, 373 (1979)
26. J. Marro, R. Dickman, *Nonequilibrium Phase Transitions in Lattice Models* (Cambridge University Press, Cambridge, 1999)
27. R. Dickman, Europhysics Lett. **61**, 294 (2003)
28. D. Dhar, P. Pradhan, J. Stat. Mech., P05002 (2004); P. Pradhan, D. Dhar, Phys. Rev. E **73**, 021303 (2006)